Ab initio Calculation of van der Waals Bonded Molecular Crystals

Deyu Lu,* Yan Li, Dario Rocca, and Giulia Galli
Department of Chemistry, University of California, Davis, Davis, California 95616, USA

(Received 23 March 2009; published 22 May 2009)

Intermolecular interactions in the van der Waals bonded benzene crystal are studied from first principles, by combining exact exchange energies with correlation energies defined by the adiabatic connection fluctuation-dissipation theorem, within the random phase approximation. Correlation energies are evaluated using an iterative procedure to compute the eigenvalues of dielectric matrices, which eliminates the computation of unoccupied electronic states. Our results for the structural and binding properties of solid benzene are in very good agreement with experimental results and show that the framework adopted here is a very promising one to investigate molecular crystals and other condensed systems bound by dispersion forces.

DOI: 10.1103/PhysRevLett.102.206411 PACS numbers: 71.15.Mb, 71.10.−w, 71.15.Nc, 71.45.Gm

van der Waals (vdW) dispersion forces play an important role in determining the physical properties of a variety of systems—including colloids and assembly of macromolecules—as well as of many fundamental processes, e.g., adhesion of liquids on surfaces [1]. Dispersion forces have a quantum mechanical nature, and they originate from fluctuations of the electronic charge density that, although nonpolar on average, may have instantaneous dipole and higher multipole moments. These long-range interactions are the dominant contribution to vdW forces for nonpolar fragments, e.g., for molecules such as benzene or methane. In the case of dipolar molecules, for example, water, vdW forces also have contributions from orientation and induction terms [2].

Theoretical descriptions of vdW dispersion forces date back to London [3] and successful theories for planar surfaces have been derived by Lifshitz [4]. However, it is only in recent years that nonempirical, quantum mechanical calculations of dispersion forces have appeared in the literature [5–11]. Accurate evaluations are very challenging [12] due to open issues in describing long-range correlation energies present in many *ab initio* theories, and to demanding computational requirements. The local density approximation (LDA) and generalized gradient approximation (GGA) to density functional theory (DFT) do not correctly describe the asymptotic behavior of dispersion interactions as a function of distance. Within DFT, progress in computing vdW forces has been recently reported by using nonlocal density functionals [6] and, for atoms and simple molecules, by computing so-called C6 coefficients from LDA and Perdew-Burke-Ernzerhof (PBE) wave functions [11]. Quantum chemistry techniques, e.g., Møller-Pleset perturbation theory and the coupled-cluster method, can describe long-range correlation effects. For example, studies of noble gas solids using a coupled-cluster approach yield cohesive energies and lattice constants within a few percent of the experiment [5]. However, applications of these quantum chemistry techniques to more complex systems, e.g., molecular crystals, are computationally very demanding and have been attempted only by using potentials fitted to computed gas-phase data [9].

In this Letter we show that an accurate and efficient description of the physical properties of molecular crystals bound by dispersion forces can be obtained from first principles, by computing correlation energies via direct evaluation of the electronic density response function. We report results for the physical properties of the benzene crystal—a prototypical vdW-bonded system—in very good agreement with experiments. Thus far, long-range correlations of the benzene crystal have been approximated either by empirical R^{-6} atomic pair potentials (even though there are several known cases for which such potentials predict qualitatively wrong asymptotic behavior of dispersion interactions [13,14]) or by using quantum-chemistry-derived pairwise dispersion potentials [9,15–17].

We employed the so-called adiabatic connection fluctuation-dissipation theorem [18] (ACFDT) to compute correlation energies, and a recently developed technique [19,20] to efficiently evaluate eigenvalues and eigenvectors of dielectric matrices. Calculations of correlation energies within the ACFDT have been reported for several systems, including jellium [21], isolated molecules [22,23], compact solids [24,25], layered materials [26], and noble gas crystals [27], and the overall good agreement with experiments indicates that the ACFDT based on either LDA or GGA is a promising approach to describe dispersion forces. However, the high computational cost involved in the standard implementations of this formalism has so far prevented its application to molecular crystals and other complex systems.

Within the ACFDT and the random phase approximation (RPA), the correlation energy is expressed as a function of the symmetrized dielectric matrix defined by $\tilde{\epsilon}_{\mathbf{G},\mathbf{G}'}(\mathbf{q}, i\omega) = \frac{|\mathbf{q}+\mathbf{G}|}{|\mathbf{q}+\mathbf{G}'|}\epsilon_{\mathbf{G},\mathbf{G}'}(\mathbf{q}, i\omega)$. In terms of eigenmodes of $\tilde{\epsilon}$, the correlation energy is given by [28,29]

$$E_c^{\mathrm{RPA}} = \frac{1}{2\pi N_q} \int_0^\infty d\omega \sum_{\mathbf{q}} \sum_j \{\log[\tilde{\epsilon}_j(\mathbf{q}, i\omega)] - \tilde{\epsilon}_j(\mathbf{q}, i\omega) + 1\}, \tag{1}$$

where $\tilde{\epsilon}_j(\mathbf{q}, i\omega)$ denotes the jth eigenvalue of $\tilde{\epsilon}$. Within a plane wave (PW) representation of the electronic states, the computational workload to evaluate $\tilde{\epsilon}$ scales as $N_v N_c N_{\mathrm{pw}}^2$, where N_v and N_c are the number of valence and conduction bands, and N_{pw} is the size of the PW basis set. As N_c is roughly equal to $N_{\mathrm{pw}} - N_v$, the standard implementation scales as $N_v N_{\mathrm{pw}}^3$. Furthermore $\tilde{\epsilon}(\mathbf{q}, i\omega)$ needs to be diagonalized in order to obtain the trace of $\log(\tilde{\epsilon})$.

In our calculations, we have replaced the direct diagonalization of the $\tilde{\epsilon}$ matrix with an iterative procedure to obtain its eigenmodes; we call such a procedure "projection of dielectric eigenpotentials" [19,20]. The action of $\tilde{\epsilon}$ on any arbitrary potential is obtained using density functional perturbation theory [30], thus eliminating the need to compute any unoccupied single particle electronic states. The cost to compute the eigenvalues of $\tilde{\epsilon}$ is reduced to $N_v^2 N_{\mathrm{pw}}^2$, making correlation energy calculations for systems with large basis sets much more affordable [19].

As a benchmark (not shown) we first applied the algorithm described above to the calculation of the exchange-correlation energy of bulk silicon, and we found results in excellent agreement with those obtained from a standard approach [25]. We then computed the bonding properties of the benzene crystal by expressing its total energy as

$$E_{\mathrm{tot}}^{\mathrm{EXX/RPA}} = (E_{\mathrm{tot}}^{\mathrm{DFT}} - E_{xc}^{\mathrm{DFT}}) + E_x^{\mathrm{EXX}} + E_c^{\mathrm{RPA}}, \tag{2}$$

where the terms on the right-hand side are the DFT total energy, DFT exchange-correlation energy, the exact exchange, and the RPA correlation energy, respectively. Although RPA exactly describes long-range correlations [31], which account for vdW interactions at long distance, it generally overestimates short-range correlations due to the lack of an exchange-correlation kernel. The RPA correlation energy with short-range corrections, referred to as RPA+ [31,32], is given by $E_{\mathrm{tot}}^{\mathrm{EXX/RPA+}} = E_{\mathrm{tot}}^{\mathrm{EXX/RPA}} + E_{sr}^{\mathrm{corr}}$, where E_{sr}^{corr} is defined as the energy difference between E_c^{LDA} (E_c^{GGA}) and the parametrized RPA correlation energy in the LDA (GGA) form. DFT calculations were carried out with the PWSCF package [33], at selected unit cell volumes. We used plane wave basis sets with a kinetic energy cutoff of 70 Ry, norm-conserving pseudopotentials, and both LDA/Perdew-Zunger [34] and GGA/PBE [35] exchange-correlation functionals. At each fixed volume, the internal geometry of the four nonequivalent monomers was fully relaxed until all ionic forces were less than 0.03 eV/Å.

The integration in imaginary frequency domain [see Eq. (1)] was carried out by 10-point Gauss-Legendre quadrature in the range of $u \in [0, 1]$, where $u = (1 + \omega/\omega_0)^{-1}$, with $\omega_0 = 1$ Hartree [36]. The eigenmode summation was evaluated by truncating j at a finite N_ϵ and fitting the correlation energy to $E_c^{\mathrm{RPA}}(N_\epsilon) = E_c^{\mathrm{RPA}}(\infty) + \alpha/N_\epsilon + \beta/N_\epsilon^2$ for a chosen range of N_ϵ.

We have checked the convergence of our results with regard to (1) the energy cutoff for the plane wave basis (E_{cut}), (2) the number of k points in the Brillouin zone of the solid phase (N_k) and the supercell size for the gas-phase molecule (a), and (3) the range of N_ϵ used in evaluating E_c^{RPA}. $E_{\mathrm{cut}} = 70$ Ry is sufficient to converge the difference between total energy of the solid and gas phase within a few tenth of kJ/mol (tests were conducted up to 120 Ry). A $2 \times 2 \times 2$ Monkhorst-Park grid of k points for the solid and a fcc supercell with size $a = 15.875$ Å for the isolated gas molecule yield converged values of $(E_{\mathrm{tot}}^{\mathrm{DFT}} - E_{xc}^{\mathrm{DFT}})$ within 0.1 kJ/mol per molecule. In the calculation of the EXX energy, the divergence in the summand for the exchange matrix element was integrated by the Gygi-Baldereschi scheme [37]. E_x^{EXX} was found to depend on the total number of k points, according to $E_x^{\mathrm{EXX}}(N_k) = E_x^{\mathrm{EXX}}(\infty) + A/N_k$, and we obtained $E_x^{\mathrm{EXX}}(\infty)$ by extrapolating from values calculated using k grids of $2 \times 2 \times 2$ and $4 \times 4 \times 4$ [38]. For gas-phase calculations, a Coulomb cutoff technique [39] was employed both in the EXX and in the projection of dielectric eigenpotentials computations, in order to remove spurious interactions between neighboring cells. As expected, relative values of E_c^{RPA} at different densities converge much faster, with respect to N_ϵ, than absolute values. The error from the truncation of N_ϵ to 500 eigenmodes is estimated to be within 1% for the equilibrium lattice constants and about 5 kJ/mol for the cohesive energy. It is interesting to note that the inclusion of only 10 eigenmodes per monomer is sufficient to recover more than 80% of the difference in correlation energy between the solid and the gas phase. However, one needs to include about 500 eigenmodes to accurately

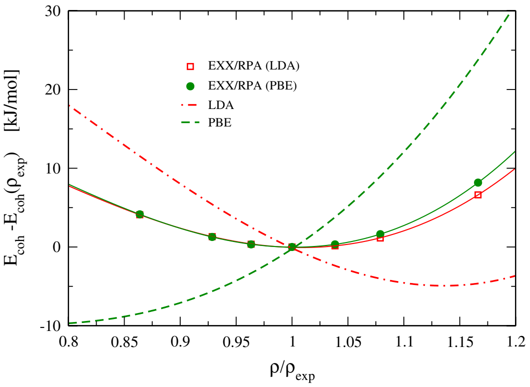

FIG. 1 (color online). Relative cohesive energy per monomer for the benzene crystal as a function of the relative density ρ/ρ_{exp} with $\rho_{\mathrm{exp}} = 8.66\ \mathrm{nm}^{-3}$ [44]. The solid lines are fitted to the third-order Birch-Murnaghan equation of state. We varied the crystal volume by isotropically scaling the lattice parameters measured from high resolution powder diffraction experiments at 4.2 K [44] (P_{bca} orthorhombic cell with $a = 7.355$ Å, $b = 9.371$ Å, and $c = 6.700$ Å).

describe the curvature of the benzene binding curve and thus obtain the equilibrium lattice constant to the accuracy reported here (an accurate comparison between gas- and solid-phase eigenmodes will be reported elsewhere).

Our results for the binding curve of the benzene crystal are presented in Fig. 1 together with those of LDA and GGA/PBE calculations and compared to experiments in Table I. LDA yields an equilibrium density about 14% larger than in experiments, while the cohesive energy (~57 kJ/mol) is close to experimental values, extracted from the measured heat of sublimation [40], and corrected for temperature effects and zero point energy [41] (see Table I). On the other hand, PBE predicts an equilibrium density about 24% smaller than in experiments and severely underbinds the crystal. These results are in close agreement with those previously reported in Ref. [42] (LDA) and [16] (PBE).

The good agreement between LDA and experiments for the binding energy originates from error cancellations, as indicated by the comparison of exchange and correlation energies between LDA and EXX/RPA (see Fig. 2): not only do the absolute values differ by a few Ry but also the energy variation as a function of the lattice constant is substantially overestimated (underestimated) in the LDA exchange (correlation) energies. The sum of the two parts (E_{xc}^{LDA}) shows instead much smaller but still appreciable (~20%) deviation from the EXX/RPA curve.

Compared to LDA, PBE exchange and correlation energies as a function of the lattice constant are in better agreement with EXX/RPA results (Fig. 2). We note that for the benzene crystal the variation in the RPA correlation energy is about the same order of magnitude as that in the EXX energy, similar to weakly bound hexagonal boron nitride layers [26], and unlike the case, e.g., of bulk Si or NaCl in which the EXX energy dominates [25] over the correlation energy.

The equilibrium density ρ_0 determined from EXX/RPA is much improved over the LDA or PBE results. The cohesive energy from EXX/RPA is smaller than in experiments by a few kJ/mol. The inclusion of short-range corrections (EXX/RPA +) shifts the binding curve up by about 2 kJ/mol, while the equilibrium lattice parameters increase by less than 1%. A larger energy difference between RPA and RPA+ was found in the case of noble gas solids (about 10%–20%) [27]. The bulk modulus B_0 from EXX/RPA+ or EXX/RPA is close to the estimated experimental value [42], and much smaller than the LDA value.

In a recent work on cohesive energy curves of noble gas solids [27], it was shown that EXX/RPA results from PBE ground states show overall similar but slightly better agreement with experiments than do those from LDA ground states, with the latter yielding smaller cohesive energies and larger lattice constants. We found the same trend for the benzene crystal: EXX/RPA binding curves calculated from PBE ground states are very similar to those from LDA ground states (see Fig. 1), but the predicted cohesive energy is increased by about 3 kJ/mol, in better agreement with experiments. We also checked the dependence of the cohesive energy on the equilibrium atomic positions by performing EXX/RPA (PBE) calculations on the LDA and PBE optimized geometries. We found that the cohesive energies differ by less than 0.05 kJ/mol.

Finally we briefly compare our results with those obtained from pair potentials derived from atomic data. We used the functional proposed by Grimme [43] and found a cohesive energy in very good agreement with experiments. However the equilibrium density is overestimated by 10%, similar to the LDA case.

In summary, we have presented a first principle study of the structural and binding properties of the benzene crystal using the ACFDT to obtain RPA correlation energies. The

TABLE I. Calculated equilibrium density $\rho_0/\rho_{\mathrm{exp}}$, cohesive energy E_{coh}, and bulk modulus B_0 of the benzene crystal from LDA, EXX/RPA (LDA), PBE, and EXX/RPA (PBE), respectively (see text). Experimental cohesive energy is from measured heat of sublimation (43–47 kJ/mol) [40], corrected for temperature effects ($2\,RT = 4.2$ kJ/mol at 250 K) and zero point energy (2.8 kJ/mol) [41].

	LDA	EXX/RPA (LDA)	PBE	EXX/RPA (PBE)	Exp.
$\rho_0/\rho_{\mathrm{exp}}$	1.14	1.01	0.76	1.00	1
E_{coh} (kJ/mol)	57.00	44.00	9.60	47.00	50–54
B_0 (GPa)	12.00	6.90	1.40	7.50	~8 [42]

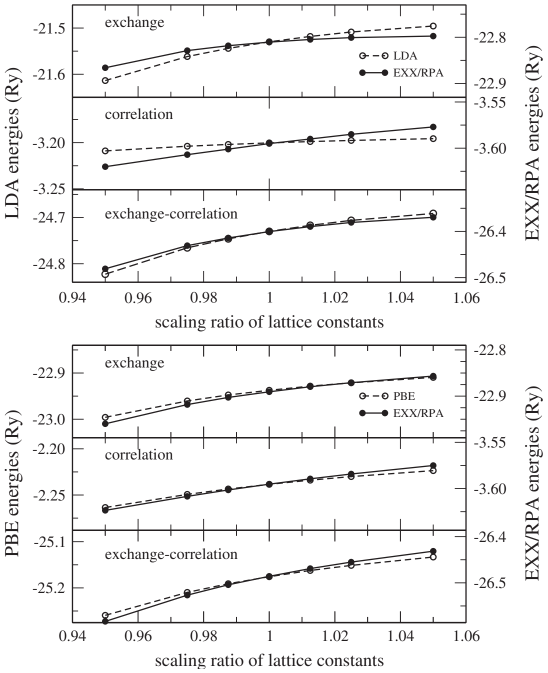

FIG. 2. Exchange and correlation energies per monomer for the benzene crystal as a function of the scaling ratio of lattice constants. LDA (PBE) and EXX/RPA results are shown by dashed and solid lines with circles, respectively.

eigenvalues of the dielectric matrix were obtained by an iterative procedure that avoids direct matrix diagonalization and calculation of electronic empty states, thus making it scalable to systems with a large number of atoms. Our framework does not necessitate the separation of the condensed system into fragments, and it does not rely on the choice of any reference system, unlike most of the dispersion-augmented DFT methods, or on the transferability to the solid phase of pair potentials computed for the gas phase. Our results are in very good agreement with experiments and indicate that the approach adopted here is a very promising one to investigate molecular crystals bound by dispersion forces, as well as self-assembled monolayers on metallic surfaces.

This work was funded by DOE/BES Grant No. DE-FG02-06ER46262 and DOE SciDAC Grant No. DE-FC02-06ER25794. Computer time was provided by NSF TeraGrid. We thank Hugh F. Wilson for benchmark EXX/RPA calculations on bulk silicon.

---

*dylu@ucdavis.edu

[1] J. N. Israelachvili, *Intermolecular and Surface Forces* (Academic Press, New York, 1991).

[2] J. N. Israelachvili and D. Tabor, Proc. R. Soc. A **331**, 19 (1972).

[3] F. London, Z. Phys. Chem. (Leipzig) **B11**, 222 (1930).

[4] I. E. Dzyaloshinskii, E. M. Lifshitz, and L. P. Pitaevskii, Adv. Phys. **10**, 165 (1961).

[5] K. Rosciszewski, B. Paulus, P. Fulde, and H. Stoll, Phys. Rev. B **60**, 7905 (1999).

[6] M. Dion, H. Rydberg, E. Schröder, D. C. Langreth, and B. I. Lundqvist, Phys. Rev. Lett. **92**, 246401 (2004).

[7] P. L. Silvestrelli, Phys. Rev. Lett. **100**, 053002 (2008).

[8] M. Rohlfing and T. Bredow, Phys. Rev. Lett. **101**, 266106 (2008).

[9] R. Podeszwa, B. M. Rice, and K. Szalewicz, Phys. Rev. Lett. **101**, 115503 (2008).

[10] D. Nabok, P. Puschnig, and C. Ambrosch-Draxl, Phys. Rev. B **77**, 245316 (2008).

[11] A. Tkatchenko and M. Scheffler, Phys. Rev. Lett. **102**, 073005 (2009).

[12] J. F. Dobson *et al.*, Australian Journal of Chemistry **54**, 513 (2001).

[13] J. F. Dobson, A. White, and A. Rubio, Phys. Rev. Lett. **96**, 073201 (2006).

[14] T. Gould, K. Simpkins, and J. F. Dobson, Phys. Rev. B **77**, 165134 (2008).

[15] E. Tapavicza *et al.*, J. Chem. Theory Comput. **3**, 1673 (2007).

[16] M. Rubes and O. Bludsky, Phys. Chem. Chem. Phys. **10**, 2611 (2008).

[17] A. L. Ringer and C. D. Sherrill, Chem. Eur. J. **14**, 2542 (2008).

[18] D. C. Langreth and J. P. Perdew, Solid State Commun. **17**, 1425 (1975); Phys. Rev. B **15**, 2884 (1977).

[19] H. F. Wilson, F. Gygi, and G. Galli, Phys. Rev. B **78**, 113303 (2008).

[20] H. F. Wilson, D. Lu, F. Gygi, and G. Galli (to be published).

[21] J. F. Dobson and J. Wang, Phys. Rev. Lett. **82**, 2123 (1999); Phys. Rev. B **62**, 10 038 (2000); J. M. Pitarke and J. P. Perdew, Phys. Rev. B **67**, 045101 (2003); J. Jung, P. García-González, J. F. Dobson, and R. W. Godby, Phys. Rev. B **70**, 205107 (2004).

[22] M. Fuchs and X. Gonze, Phys. Rev. B **65**, 235109 (2002); F. Aryasetiawan, T. Miyake, and K. Terakura, Phys. Rev. Lett. **88**, 166401 (2002); M. Fuchs, K. Burke, Y.-M. Niquet, and X. Gonze, Phys. Rev. Lett. **90**, 189701 (2003); F. Aryasetiawan, T. Miyake, and K. Terakura, Phys. Rev. Lett. **90**, 189702 (2003); F. Furche and T. V. Voorhis, J. Chem. Phys. **122**, 164106 (2005); J. Toulouse, I. C. Gerber, G. Jansen, A. Savin, and J. G. Ángyán, Phys. Rev. Lett. **102**, 096404 (2009).

[23] H.-V. Nguyen and S. de Gironcoli, arXiv:0902.0889v2 [Phys. Rev. B (to be published)].

[24] T. Miyake *et al.*, Phys. Rev. B **66**, 245103 (2002).

[25] P. Garcia-Gonzalez, J. J. Fernandez, A. Marini, and A. Rubio, J. Phys. Chem. A **111**, 12 458 (2007).

[26] A. Marini, P. Garcia-Gonzalez, and A. Rubio, Phys. Rev. Lett. **96**, 136404 (2006).

[27] J. Harl and G. Kresse, Phys. Rev. B **77**, 045136 (2008).

[28] Y. M. Niquet, M. Fuchs, and X. Gonze, Phys. Rev. A **68**, 032507 (2003).

[29] In order to derive Eq. (1) from Eq. (10) in Ref. [28], one recognizes that the trace is similarity invariant; i.e., $\mathrm{Tr}(\chi_0 v) = \mathrm{Tr}(v^{1/2}\chi_0 v^{1/2}) = \mathrm{Tr}(1 - \tilde{\epsilon})$, where $v = v^{1/2}v^{1/2}$ is the Coulomb kernel. Since $\tilde{\epsilon}(i\omega)$ is Hermitian, Eq. (1) is obtained by evaluating the trace as the sum of eigenvalues.

[30] S. Baroni, S. de Gironcoli, A. Dal Corso, and P. Giannozzi, Rev. Mod. Phys. **73**, 515 (2001).

[31] S. Kurth and J. P. Perdew, Phys. Rev. B **59**, 10 461 (1999).

[32] Z. Yan, J. P. Perdew, and S. Kurth, Phys. Rev. B **61**, 16 430 (2000).

[33] P. Giannozzi *et al.*, http://www.quantum-espresso.org.

[34] J. P. Perdew and A. Zunger, Phys. Rev. B **23**, 5048 (1981).

[35] J. P. Perdew, K. Burke, and M. Ernzerhof, Phys. Rev. Lett. **77**, 3865 (1996).

[36] The final value of the quadrature is insensitive to the choice of ω_0 in a reasonable range. The difference between calculations performed with 10- and 20-point Gauss-Legendre quadrature is negligible.

[37] F. Gygi and A. Baldereschi, Phys. Rev. B **34**, 4405 (1986).

[38] The scaling factor A is about 0.1 Ry per monomer for cell volumes considered in this work. The error involved in the evaluation of E_x^{EXX} using only a $2 \times 2 \times 2$ k grid is estimated to be about 20 kJ/mol for the cohesive energy and 3%–4% for the equilibrium density; this highlights the importance of accurately converging the EXX energy with respect to N_k.

[39] C. A. Rozzi, D. Varsano, A. Marini, E. K. U. Gross, and A. Rubio, Phys. Rev. B **73**, 205119 (2006).

[40] J. S. Chickos and W. E. Acree, Jr., J. Phys. Chem. Ref. Data **31**, 537 (2002).

[41] M. Nakamura and T. Miyazawa, J. Chem. Phys. **51**, 3146 (1969).

[42] E. J. Meijer and M. Sprik, J. Chem. Phys. **105**, 8684 (1996).

[43] S. Grimme, J. Comput. Chem. **27**, 1787 (2006).

[44] W. David, R. Ibberson, G. Jeffrey, and J. Ruble, Physica (Amsterdam) **180–181B**, 597 (1992).